Journal of Physiology (1992), **451**, *pp.* 187–203
With 7 figures
Printed in Great Britain

CALCIUM CURRENT ACTIVATION AND CHARGE MOVEMENT IN DENERVATED MAMMALIAN SKELETAL MUSCLE FIBRES

BY OSVALDO DELBONO

From the Department of Molecular Physiology and Biophysics, Baylor College of Medicine, Houston, TX 77030, USA

(*Received 5 July 1991*)

SUMMARY

1. Calcium current (I_{Ca}) activation was studied in denervated extensor digitorum longus muscle fibres of the rat. Denervation was performed by surgically removing 6–8 mm of the sciatic nerve at the sciatic notch. Controls were normal fibres from non-operated rats. Electrical recordings were carried out using the double Vaseline-gap technique.

2. Current–voltage (I–V) curves showed that the I_{Ca} amplitude increased during the first 4–6 days after denervation and subsequently decreased during the second week. Between days 4 and 6 after denervation, the peak I_{Ca} amplitude (at 0 mV) was $-5{\cdot}9 \pm 0{\cdot}5$ μA/μF (mean ± S.E.M.) as compared with $-4{\cdot}8 \pm 0{\cdot}3$ μA/μF in normal fibres. Between days 14 and 15 after denervation, the I_{Ca} amplitude was $-2{\cdot}9 \pm 0{\cdot}4$ μA/μF.

3. The time constant of I_{Ca} activation (τ_a) was significantly increased by denervation. At 0 mV, τ_a in normal fibres was $44{\cdot}8 \pm 1{\cdot}4$ ms. Between 4 and 6 days after denervation τ_a was $58{\cdot}1 \pm 4{\cdot}8$ ms, and between 14 and 15 days after denervation, $55{\cdot}8 \pm 3{\cdot}8$ ms.

4. The time constant of deactivation (τ_d) decreased after denervation. At -10 mV, the τ_d in normal fibres was $103{\cdot}4 \pm 14$ ms. The value decreased to $74{\cdot}5 \pm 8{\cdot}6$ and $74{\cdot}0 \pm 17$ ms between days 4 and 6 and days 14 and 15 of denervation respectively.

5. Charge movement (Q_{on}) was reduced progressively without major changes in the steepness (k) and position on the voltage axis of the Q_{on}–V_m relationship. The fitted parameters under control were $Q_{max} = 15{\cdot}4$ nC/μF, mid-point potential $V_{q\frac{1}{2}} = -25{\cdot}2$ mV and $k = 11{\cdot}9$ mV. Between days 14 and 15 of denervation, the values for Q_{max}, $V_{q\frac{1}{2}}$ and k were 6·7 nC/μF, $-36{\cdot}8$ mV and 11·3 mV respectively.

6. Calcium permeability (P_{Ca}) in normal and denervated fibres at stages during denervation was calculated according to the Hodgkin–Huxley model. At 0 mV P_{Ca} was $1{\cdot}24 \times 10^{-5}$ cm/s in normal fibres, and $7{\cdot}43 \times 10^{-6}$ cm/s after 2 weeks of denervation.

7. The m_∞–V_m relationship was shifted to more positive potentials after denervation without significant changes in the steepness factor k. The $V_{\frac{1}{2}}$ value in normal fibres was $-4{\cdot}4$ mV, and 5·8 mV after two weeks of denervation.

8. The I_{Ca} sensitivity to nifedipine was not modified in the different groups of denervated fibres studied. With 10 μM-nifedipine, the $1-(I_{Ca}$ in nifedipine/I_{Ca}

control) relationships were $0{\cdot}74 \pm 0{\cdot}03$ in normal fibres and $0{\cdot}76 \pm 0{\cdot}12$, 14 days after denervation.

INTRODUCTION

Several changes occur when the nerve–skeletal muscle connection is interrupted. Contractile properties are modified after denervation (Gutmann & Sandow, 1965; Finol, Lewis & Owens, 1981; Lorkovik, 1985). Electrical changes also occur after denervation as a consequence of expression of new channels, alterations in sarcolemmal ionic permeabilities and currents (Pappone, 1980; Schmid-Antomarchi, Renaud, Romey, Hugues, Schmid & Lazdunski, 1985; Henderson, Lechleiter & Brehm, 1987; Kotsias & Venosa, 1987; Gonoi & Hasegawa, 1988; Conte Camerino, De Luca, Mambrini, Vrbova, 1989) and development of ionic channels resistant to their usual blockers (Harris & Thesleff, 1971; Pappone, 1980; Duval & Leoty, 1985; Guo, Bryant & Moczydlowski, 1986; Weiss & Horn, 1986).

A major characteristic of denervated muscles is the inability to sustain tension during prolonged contractions such as tetanus contraction and potassium contracture (Finol *et al.* 1981; Dulhunty & Gage, 1985; Lorkovic, 1985; Obejero Paz, Delbono & Muchnik, 1986) although this is not the case in prolonged contracture such as that induced by caffeine (Gutmann & Sandow, 1965). Therefore a voltage-dependent mechanism may be involved in failure to sustain prolonged contraction. In agreement with this, failure in repetitive electrical activity could account for the decrease in denervated fibre mechanical output (Kotsias & Muchnik, 1987). However, there may be more than one underlying mechanism. It is possible that a voltage-dependent process involved in prolonged skeletal muscle contraction, such as the dihydropyridine (DHP)-sensitive I_{Ca} through L-type channels (Cota & Stefani, 1981), may be altered after mammalian fibre denervation. It is possible that an alteration of Ca^{2+} flux through these channels, a modification of the channel structure, regarded as the same molecules as the voltage sensors (Ríos & Brum, 1987), or a decrease in Ca^{2+} channel density underlie the mechanical failure in denervated muscle.

In a previous work we demonstrated that calcium action potentials were substantially decreased after two weeks of denervation of rat extensor digitorum longus (Delbono & Kotsias, 1991). In normal fibres the incidence of calcium action potentials reached more than 90%, and only 14% in fibres 14–15 days after denervation. The present study is designed to determine whether there is an actual reduction of I_{Ca} in denervated fibres, or whether this effect is due to a shunting of this current by an outward K^+ current.

Part of these results was presented at the Biophysical Society Meeting (Delbono, García & Stefani, 1991*b*).

METHODS

Denervation and fibre preparation. Denervation of Wistar rats was carried out by removing 5–8 mm of the right sciatic nerve just distal to the sciatic notch under a rodent cocktail (42·8 mg ketamine, 8·6 mg xylazine and 1·4 mg acepromazine per millilitre; dose, 0·5–0·7 ml/kg I.M.) in addition to ether anaesthesia. The animals were allowed to recover from the anaesthetic and were maintained for periods from 4 to 21 days. Extensor digitorum longus (EDL) muscle was dissected after the rat was killed in a carbon dioxide chamber. Denervated muscles exhibited fibrillations, lack of mechanical response to the stimulation of the distal portion of the nerve and complete

absence of reinnervation or persistence of colateral innervation. Controls were normal fibres from non-operated rats. These rats were also killed in a CO_2 chamber. The muscles were kept for 8–9 h in a beaker containing Ringer–Krebs solution (see Table 1, Delbono, García, Appel & Stefani, 1991*a*). A bundle of muscle fibres was excised and transferred to a chamber filled with 'dissecting

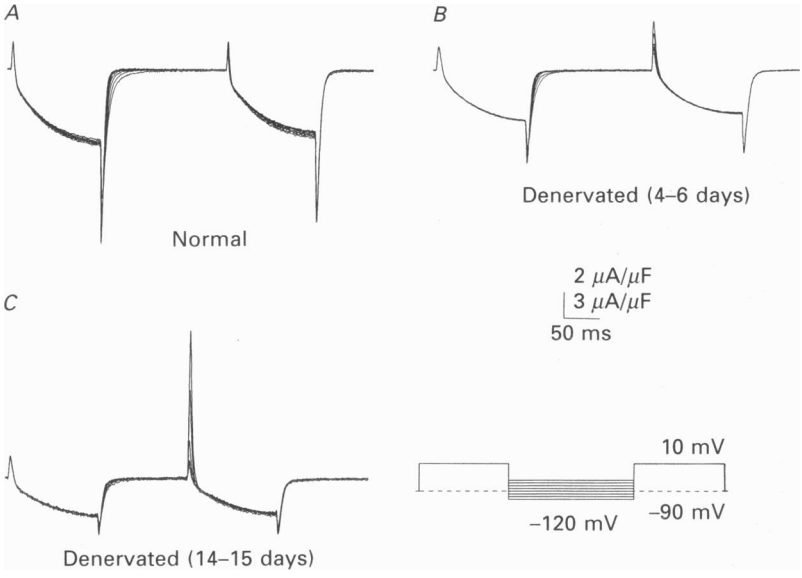

Fig. 1. I_{Ca} recordings in normal (*A*), 5-day-denervated (*B*), and 14-day-denervated fibres (*C*) obtained by applying the pulse protocol depicted on the lower right part of the figure. Two test pulses of 150 ms duration to 10 mV were applied, the first from V_h −90 mV, and the second from V_h −50 to −120 mV. The vertical calibration bar corresponds to 2 μA/μF for *A* and *C*, and 3 μA/μF in *B*.

solution', where single fibres were manually dissected under the microscope. The electrical recordings were performed using the double Vaseline-gap technique, similar to the one introduced by Kovács, Ríos & Schneider (1983) and modified by Francini & Stefani (1989). Fibres with small radius were selected to reduce tubular-clamp non-uniformities (Sánchez & Stefani, 1983). The diameter of normal and denervated fibres are indicated in Table 1. Agar bridges, equilibrated with 1 M-KCl, provided electrical connections between each compartment and separate wells that were filled with 3 M-KCl and fitted with Ag–AgCl pellets. It was possible to switch from voltage-pulse to voltage-clamp mode as was described previously (Francini & Stefani, 1989; Delbono *et al.* 1991*a*). In the voltage-clamp mode, the command pulses referred to ground were applied at the central pool. The current was injected into one of the end pools (I) via a variable gain feedback amplifier. The negative input of the amplifier was connected to the other end pool (E). Membrane potential (V_m) was measured between the middle pool and the compartment E, and the current as the voltage drop across a 100 kΩ resistance. In the voltage-pulse mode, voltage pulses were applied to compartment I and the feedback amplifier was connected to ground. Passive properties were measured according to Irving, Maylie, Sizto & Chandler (1987), with the voltage clamp and the voltage pulse mode at 0 mV and −90 mV. The membrane potential was held at −90 mV. Holding current ranged between −15 and −30 nA and was stable throughout the experiment. Fibres survived for about 2–3 h. Steady-state current-to-voltage ratio in voltage-pulse mode was used to calculate the apparent input conductance of the fibre. The capacitance of the fibres was calculated from the integral of the current transients and the amplitude of the voltage step applied in the voltage-clamp mode. The following passive properties parameters were calculated for each fibre: r_m (fibre membrane resistance for unit length), r_i (internal resistance per unit length), r_e (the external resistance under the Vaseline seal), R_m (specific membrane resistance), R_i (specific internal resistance). The ratio $r_e/(r_e+r_i)$ reflects the quality of the Vaseline seals.

Solutions. The fibres were dissected and mounted using 'dissecting' and 'mounting solutions'

(see Table 1, Delbono *et al.* 1991*a*). Single fibres were dissected in a depolarizing and low-Ca^{2+} solution in such a way that damage during the dissection could be easily visualized. The mounting solution had 1 mM-EGTA to avoid fibre contraction in the transferring manoeuvre from the dissecting to the recording chamber (both solutions were buffered at pH 7·2 ± 0·05. We added 9-anthracenecarboxylic acid (1 mM), tetrodotoxin (TTX, 1 μM) and 3,4-diaminopyridine (3,4-DAP, 1 mM) to the external solution. Osmolarity of both internal and external solutions were critically adjusted prior to the experiments to prevent fibre detubulation (300 ± 10 mosmol/l). Solution replacement (95%) in the recording pool (E) was achieved by perfusing 1 ml of the test solution in 5–20 s. Nifedipine experiments were performed in red dark light. The final nifedipine concentration was prepared by adding the drug from a 10 mM stock solution in ethanol. The bath temperature was 17 °C and was controlled (± 0·2 °C) by a Peltier system and a thermistor. The temperature was recorded with a probe located close to the middle portion of the fibre.

Stimulation, recording and data analysis. For data acquisition, stimulation and analysis an IBM AT personal computer was used. D/A and A/D conversion, 12 bits, were implemented by a Labmaster Interface (Scientific Solutions Inc., Solon, OH, USA). Membrane current during a voltage pulse, P, was initially corrected by analog subtraction of linear components. The remaining linear components were digitally subtracted by automated scaling of control pulses which were $-\frac{1}{4}$ of P. The following stimulating protocols were used: (a) *activation*, 0·3 s depolarizing pulses from holding potential (V_h) of −90 in 10 mV increments to 30 mV; (b) *charge movement*, 0·05 s depolarizing pulses from V_h −90 mV in 10 mV increments to 30 mV; (c) *double pulse with variable interpulse holding potential* (see below). Electrical signals were filtered at 0·3 of the sampling frequency (−3 dB point) with a four-pole Butterworth low-pass filter (Frequency Devices, Inc., Haverhill, MA, USA). Membrane currents are expressed per membrane capacitance (amperes per farad). Values are given as means ± S.E.M. with the number of observations (n). Data were stored in optic disc for subsequent analysis.

Denervation test in single fibres. Denervated and non-denervated fibres can be distinguished by applying a double test pulse (150 ms duration) in the presence of I_{Ca} recording solutions. The first was from V_h −90 mV, and the second was from V_h −50 to −120 mV (*double pulse with variable interpulse holding potential protocol*). Figure 1 shows three groups of traces in a normal fibre (*A*), in a fibre at day 4 after denervation (*B*), and in another fibre at day 15 of denervation (*C*). Each test pulse gave rise to an initial upward deflection that corresponded to the charge movement, followed by a downward deflection that corresponded to the activation of the DHP-sensitive I_{Ca}. At the end of the pulses a large inward Ca^{2+} tail current was recorded due to the increase in Ca^{2+} driving force. As can be seen, a large outward current was superimposed on the second charge movement records in 4- to 6-day-denervated fibres (*B*) and even larger in fibres denervated for 2 weeks (*C*). This current was not seen in normal fibres. This outward current corresponded to the activation of TTX-resistant Na^+ channels (1 μM-TTX). A similar current can be observed in normal fibres in the absence of TTX. This current was carried by Na^+, since it became undetectable when internal Na^+ was replaced by Cs^+. The negative prepulse was necessary to record the TTX-resistance Na^+ current since as a consequence of denervation Na^+ current inactivation was shifted towards more negative membrane potentials (Pappone, 1980) (see Discussion). This pulse protocol was applied at the beginning of the experiment to confirm denervation. Most of the records were obtained at a holding potential of −90 mV, a condition in which this outward current did not become prominent due to inactivation.

Denervated fibres were divided into four groups: (a) 4–6 days, (b) day 7, (c) 8–13 days and (d) day 14.

RESULTS

Passive electrical properties

The r_m, r_i and r_e (see Methods) were calculated for each muscle fibre. In the voltage-pulse mode, we initially measured the membrane potential while that I pool was disconnected (Delbono *et al.* 1991*a*). Typical values ranged between −15 and −30 mV. After this, a 20 mV voltage pulse was applied to the I end, which was recorded as a fraction of this potential (−17 to −20 mV), between the central and the other pool. This measurement reflects the adequacy of the seal resistance in

relation to the longitudinal myoplasmic and transverse membrane resistances. The membrane was then polarized to −90 mV.

The input capacitance in normal fibres was 5·58±0·3 nF ($n = 30$) and the specific membrane capacitance was 10·4±0·95 μF/cm^2 ($n = 30$). Between days 4 and 6 of denervation the diameter of the fibres slightly increased. In accordance with change,

TABLE 1. Passive electrical properties

Fibre type	d (m)	IC (nF)	C_m (F/cm^2)	R_m Ω cm^2	R_i Ω cm	$r_e/(r_e+r_i)$
Normal	53·7 (±2·9)	5·58 (±0·30)	10·4 (±0·95)	6355 (±1154)	367 (±17)	0·974 (±0·011)
Denervated (days)						
4–6	57·3 (±3·2)	6·31 (±0·56)*	19·8 (±0·97)*	5723 (±867)	407 (±46)	0·986 (±0·031)
7	49·7 (±4·6)	5·10 (±0·37)	16·4 (±0·92)*	5423 (±645)	340 (±67)	0·969 (±0·027)
8–13	38·0 (±2·3)	3·93 (±0·57)*	12·7 (±0·95)*	6123 (±1123)	418 (±59)	0·992 (±0·041)
14–15	25·6 (±5·7)*	3·30 (±0·41)*	11·6 (±1·16)*	6007 (±725)	391 (±49)	0·947 (±0·058)

The number of fibres studied were thirty normal and ten fibres for each group of denervation. The variables are: d, fibre diameter; IC, input capacitance; C_m, specific membrane capacity; R_m, specific membrane resistance; R_i, specific internal resistance; $r_e/(r_e+r_i)$, ratio between external resistance (r_e) and the sum of r_e and the internal resistance (r_i) per unit length. Values are means (±S.E.M.). *$P < 0·05$ (Student's t test, unpaired data).

the input capacitance (IC) and the specific membrane capacity (C_m) also increased in a significant way. During the second week of denervation the fibre diameter was lower than in control (close to one-half of control values) and in a parallel manner to the IC, the membrane capacitance initially increased and then decreased, but the values were always higher than under control (normal fibres; Table 1). This is only in agreement with Dulhunty & Gage (1985) if the input capacitance is expressed per membrane surface (C_m). The values of r_m, r_e and r_i, were derived from the measurements mentioned above and were used to calculate: R_m, R_i and the ratio $r_e/(r_e+r_i)$. R_m had a value of 6355±1154 Ω cm^2 ($n = 30$); this value is similar to that reported for frog skeletal muscle fibres in a similar solution (6363 Ω cm^2; Irving *et al.* 1987). The value of R_i was 367±17 Ω cm. This value is somewhat greater than that reported for the frog (214 Ω cm; Irving *et al.* 1987). The calculated ratio $r_e/(r_e+r_i)$ was 0·974±0·011. This value was very close to 1, indicating the adequacy of this method for membrane current measurements in mammalian skeletal muscle. The values of R_m, R_i and $r_e/(r_e+r_i)$ ratio at stages during denervation were not different compared to those in normal fibres.

I_{Ca}–voltage relationship at stages during denervation

Figure 2*A–E* shows I_{Ca} traces in normal and denervated fibres. All traces were normalized per membrane capacity in order to compare changes in I_{Ca} amplitude during different denervation periods. I_{Ca} amplitude increased during the first denervation period (4–6 days) without modification of the potential at which I_{Ca} was

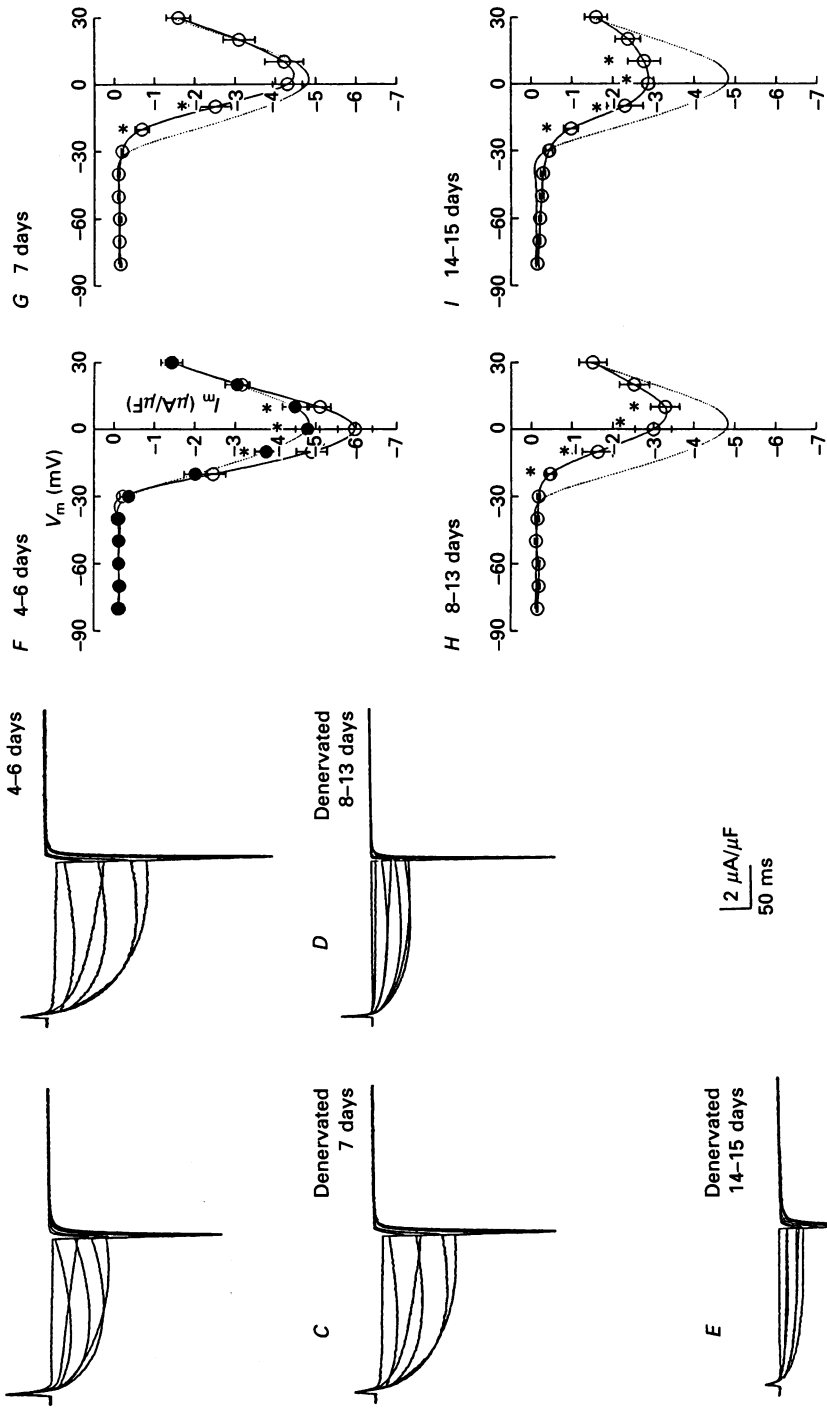

Fig. 2. *A–E* show a group of I_{Ca} recordings at stages during denervation (from 4 to 15 days). The records were obtained by applying the *activation* pulse protocol. Traces from −30 to 20 mV are shown. Right panels (*F–I*) show *I–V* curves in normal fibres (●) and 4- to 6-day-denervated fibres (○) (*F*), at day 7 of denervation (*G*), between 8 and 13 days after denervation (*H*) and between 14 and 15 days after denervation (*I*). Only the smoothed curve of normal fibres is depicted from *G* to *I*. *mark statistically significant differences ($P < 0{\cdot}05$).

activated (−30 mV). Only traces from −30 to 20 mV are shown. At day 7 of denervation the I_{Ca} amplitude was not different compared to control, and after that day, the peak I_{Ca} decreased to about 40% of that of normal fibres between days 14 and 15. The *I–V* relationships are represented in Fig. 2 *F–I*. The values of normal

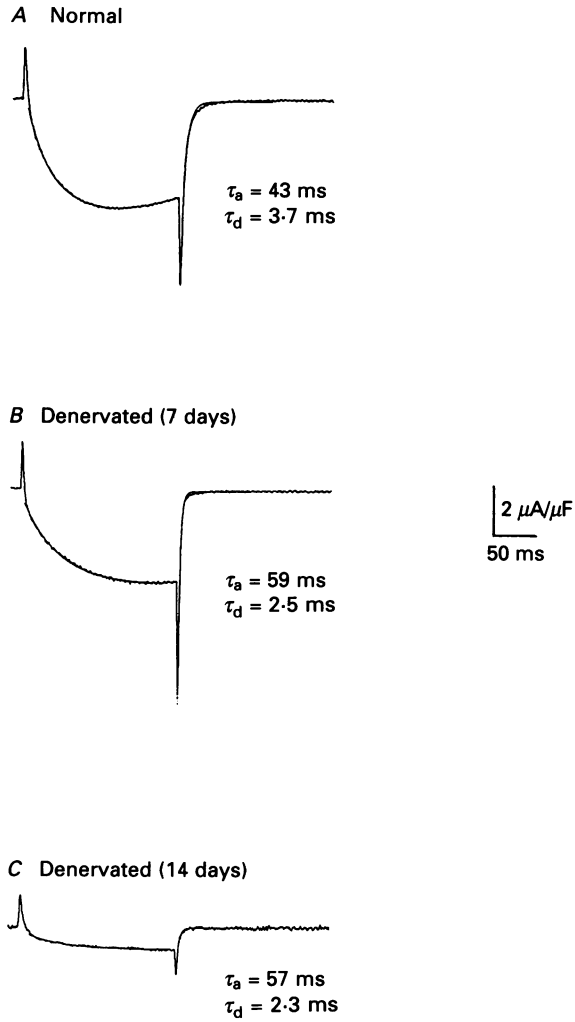

Fig. 3. I_{Ca} recordings in normal (*A*), and at days 7 (*B*) and 14 (*C*) after denervation at 0 mV (V_h −90 mV). The three records have the fitted curves to I_{Ca} activation (τ_a) and deactivation (τ_d) superimposed. The values of τ_a and τ_d correspond to each particular fibre. The fitted curves were calculated from the beginning of the pulse to a steady-state or peak I_{Ca} value and from the end of the pulse to a steady-state I_{Ca} value at −90 mV.

fibres (●, *F*) are in agreement with data from Delbono *et al.* (1991*a*). Between days 4 and 6 after denervation (○), the I_{Ca} amplitude significantly increased in the potential range between −10 and 10 mV. At 0 mV, where the maximal I_{Ca} was recorded, the value was $-4{\cdot}8 \pm 0{\cdot}3$ μA/μF ($n = 51$) and in denervated fibres $-5{\cdot}9 \pm 0{\cdot}5$ μA/μF ($n = 10$). At day 7 the difference was not significant (*G*). At 0 mV, the peak I_{Ca} value was $-4{\cdot}72 \pm 0{\cdot}56$ μA/μF ($n = 10$). In the third group of

denervated fibres (8–13 days) the I_{Ca} amplitude was significantly lower than in normal fibres within the −20–10 mV range of potentials. Between 0 and 10 mV, the maximal value of $-3{\cdot}3 \pm 0{\cdot}5$ μA/μF (10 mV; $n = 10$; *H*) was reached. Between days 14 and 15 of denervation the I_{Ca} amplitude was lower than in the third group ($-2{\cdot}9 \pm 0{\cdot}4$ μA/μF, at 0 mV, $n = 10$).

Time constants of I_{Ca} activation (τ_a) and deactivation (τ_d)

Figure 3 shows three I_{Ca} traces in fibres which were normal (*A*), denervated for 7 days (*B*), and denervated for 14 days (*C*). The rising phase of mammalian skeletal muscle fibres I_{Ca} can be adequately fitted to a single-exponential function (Mejía-Alvarez, Fill & Stefani, 1991; Delbono *et al.* 1991*a*). The fitting to I_{Ca} activation and deactivation was superimposed to each trace. τ_a was determined by fitting the current trace to an exponential function from the beginning of the pulse to the point where the current reached a steady-state level. τ_d was calculated by fitting the same function to the tail I_{Ca} from the end of the pulse to the steady state of the current after returning to −90 mV. During denervation (7 and 14 days), τ_a was increased, while τ_d at this potential (−90 mV) was not modified.

Figure 4 (*A–D*) shows the τ_a–V_m relationship. At 0 mV τ_a were as follows (in ms): in normal fibres, $44{\cdot}8 \pm 1{\cdot}4$ ($n = 10$); between 4 and 6 days of denervation, $58{\cdot}1 \pm 4{\cdot}8$ (*A*); at day 7, $59{\cdot}4 \pm 4{\cdot}8$ ($n = 10$) (at −10 mV τ_a was $70{\cdot}5 \pm 7{\cdot}0$) (*B*); between 8 and 13 days, $50{\cdot}0 \pm 5{\cdot}0$ (*C*); and between 14 and 15 days, $55{\cdot}8 \pm 3{\cdot}8$ ($n = 10$) (*D*). In summary, the activation time constant was increased in the four groups of denervation.

Figure 4 (*E–H*) shows the τ_d–V_m relationship at stages during denervation. At −10 mV τ_d were as follows (in ms): $103{\cdot}4 \pm 14$ in normal fibres; $74{\cdot}5 \pm 8{\cdot}6$ between 4 and 6 days of denervation (*E*); $46 \pm 8{\cdot}7$ at day 7 (*F*); 58 ± 19 between 8 and 13 days (*G*) and $74{\cdot}0 \pm 17$ between 14 and 15 days (*H*).

Charge movement in denervated fibres

Figure 5*A* shows a group of charge movement traces in normal fibres, and at stages of denervation (4–15 days). All these records were obtained applying the *charge movement* protocol in I_{Ca} recording solutions. I_{Ca} records were digitally subtracted with the sloping baseline procedure. Figure 5*B–E* shows the Q_{on}–V_m relationship at different days after denervation, where Q_{on} is the charge during the pulse. Control values are represented by ●. Experimental data were fitted to a single Boltzmann equation:

$$Q_{on} = Q_{max}/(1+\exp((V_{q\frac{1}{2}}-V)/k)), \quad (1)$$

where Q_{max} is the maximum charge moved, $V_{q\frac{1}{2}}$ is the mid-point potential of the curve, and k is the steepness of the curve. In control, the Q_{on}–V_m relationship was better fitted with the following parameter values: $Q_{max} = 15{\cdot}4$ nC/μF, $V_{q\frac{1}{2}} = -25{\cdot}2$ mV and $k = 11{\cdot}9$ mV. Between 4 and 6 days of denervation, this relationship was shifted to more negative potentials. The differences were statistically significant at −30 and −20 mV($Q_{max} = 13{\cdot}9$ nC/μF, $V_{q\frac{1}{2}} = -38{\cdot}4$ mV and $k = 9{\cdot}0$ mV) (see Fig. 5*B*). At day 7 of denervation, there was a clear reduction of the charge moved, particularly at potentials more positive than −10 mV, where the difference was significant. The fitted parameters at this day 7 denervation stage

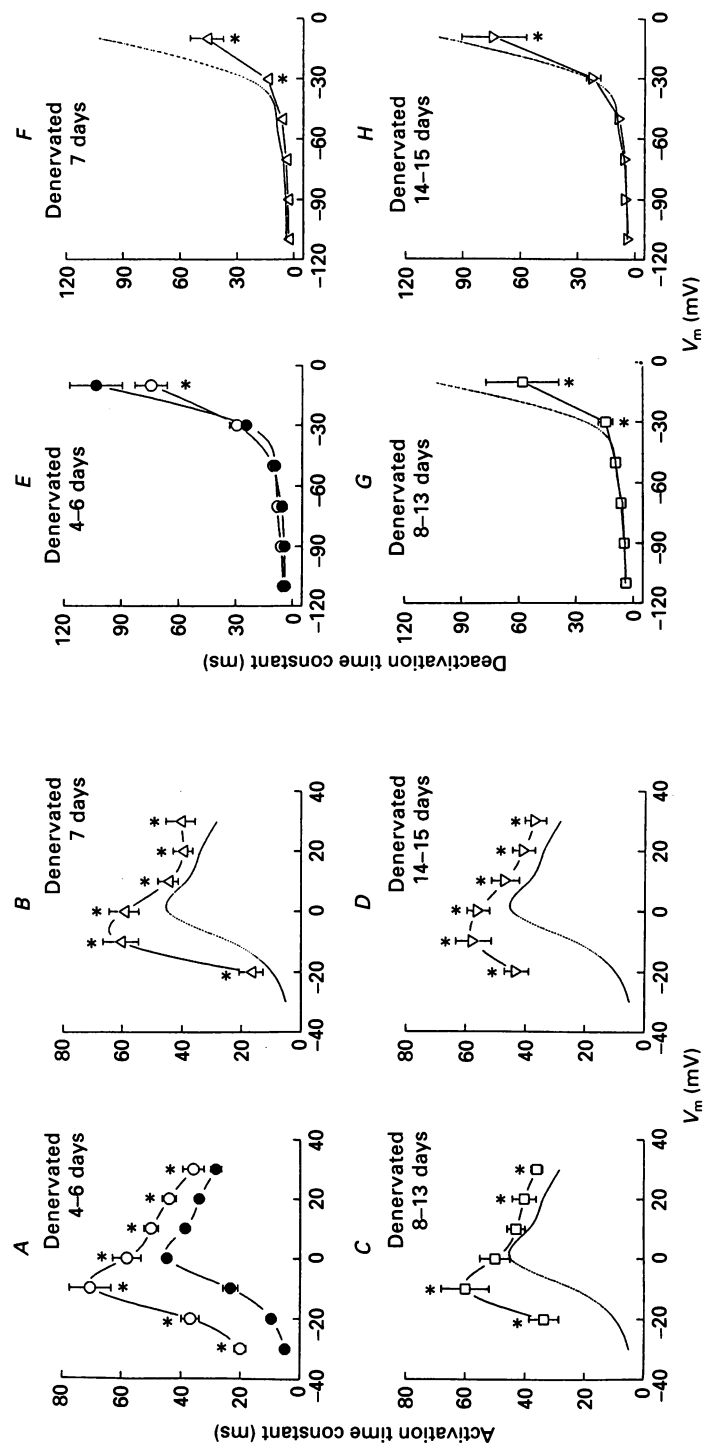

Fig. 4. Activation time constant–V_m relationship in normal fibres (●) and at different stages during denervation (open symbols; *A–D*). Deactivation time constant–V_m relationship in normal fibres (●) and during denervation (open symbols; *E–H*). Only the smoothed curve of normal fibres is depicted. Asterisks mark statistically significant differences ($P < 0{\cdot}05$).

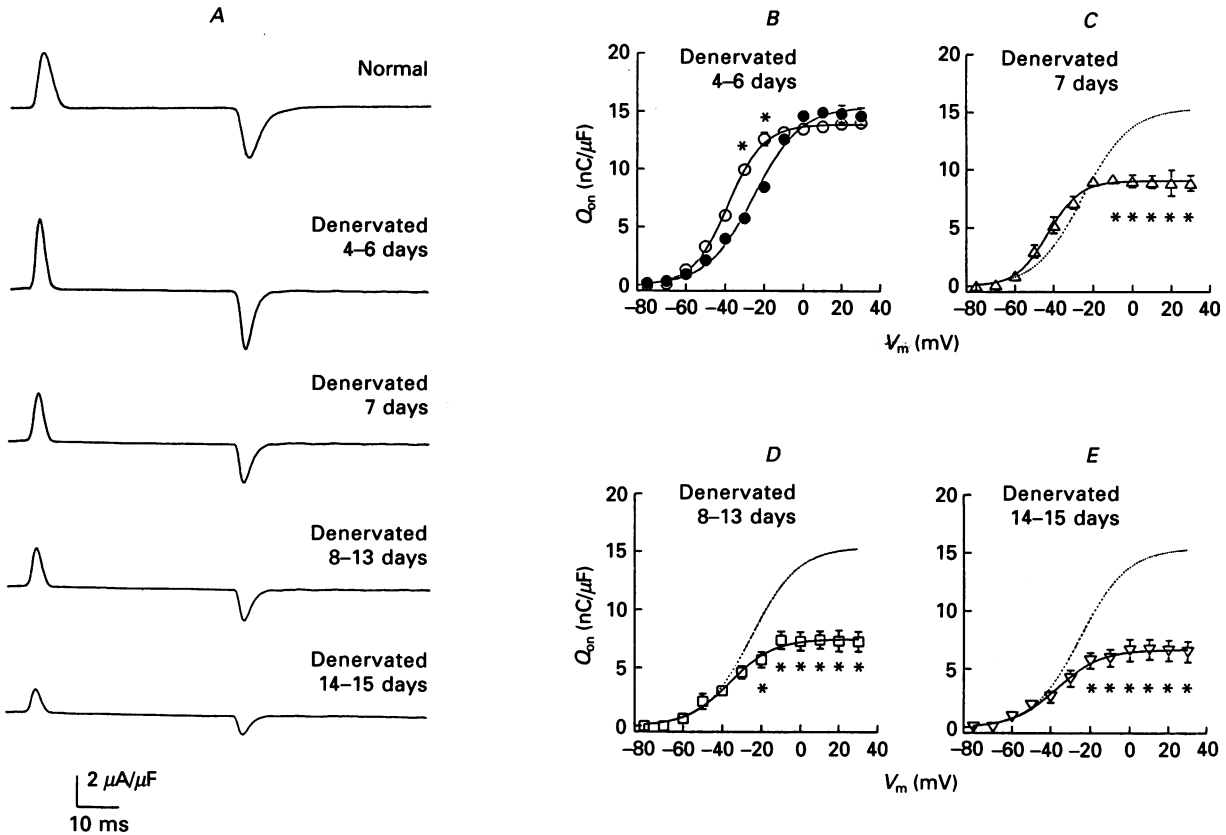

Fig. 5. *A*, charge movement traces at 0 mV obtained with the *charge movement* pulse protocol in normal and denervated fibres. *B–E* show Q_{on}–V_m relationship in normal fibres (●) and at various stages after denervation (open symbols). Experimental points were fitted to a single Boltzmann equation. The fitted curve to the control values is depicted (*C–E*). Asterisks mark statistically significant differences ($P < 0.05$).

were $Q_{max} = 9{\cdot}1$ nC/μF, $V_{q\frac{1}{2}} = -42{\cdot}9$ mV, and $k = 8{\cdot}2$ mV (*C*). Between days 8 and 13 of denervation the reduction of the charge movement was even more pronounced. The fitted parameters were $Q_{max} = 7{\cdot}5$ nC/μF, $V_{q\frac{1}{2}} = -36{\cdot}0$ mV and $k = 11{\cdot}1$ mV. The reduction of the charge movement was significant from -20 mV to more

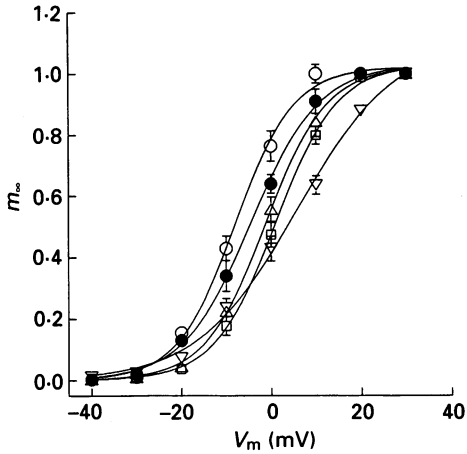

Fig. 6. The m_∞–V_m relationship in normal and denervated fibres. The experimental points were fitted to a single Boltzmann equation. For the fitted parameters, see text. ●, normal; ○, denervated 4–5 days; △, 7 days; □, 8–13 days; ▽, 14 days.

positive potentials (*D*). Between days 14 and 15 of denervation (*E*), the fitted curve to the experimental data was very similar to that obtained with the previous group. The values of Q_{max}, $V_{q\frac{1}{2}}$ and k, were 6·7 nC/μF, $-36{\cdot}8$ and 11·3 mV respectively.

I_{Ca} activation parameters

The model and terminology introduced by Hodgkin & Huxley (1952) was employed to obtain the kinetics parameters of I_{Ca} activation and inactivation. Following previous procedures (Reuter & Scholz, 1977; Sánchez & Stefani, 1983), the Goldman–Katz equation for the instantaneous I–V_m relationship for Ca^{2+} channels of rat skeletal muscle is assumed:

$$I_{Ca} = (4F^2V_m P_{Ca}[Ca^{2+}]_o (\exp(2F(V_m - V_{mCa})/RT))/(RT \exp(2FV_m/RT) - 1), \quad (2)$$

where F, R and T have their usual thermodynamic meanings, $[Ca^{2+}]_o$ is the external Ca^{2+} concentration, V_m is the membrane potential, V_{mCa} is the reversal potential of I_{Ca} and was assumed to be 150 mV, and P_{Ca} is the Ca^{2+} permeability. For these calculations, the peak I_{Ca} values were not corrected by the inactivation since the latter is a much slower process. The voltage dependence of Ca^{2+} activation (P_{Ca}) can be expressed as: $P_{Ca} = P_{Ca}\, m_\infty$ (3), where P_{Ca} is the limiting Ca^{2+} permeability and m_∞ is the steady-state activation curve. From eqn (1), P_{Ca} values at different membrane potentials (V_m) are solved. P_{Ca} at 0 mV was $1{\cdot}24 \times 10^{-5}$ cm/s in control conditions. The P_{Ca} values were $1{\cdot}55 \times 10^{-5}$, $1{\cdot}11 \times 10^{-5}$, $7{\cdot}77 \times 10^{-6}$ and $7{\cdot}43 \times 10^{-6}$ cm/s between 4 and 6 days of denervation, at day 7, between 8 and 13 days and between 14 and 15 days of denervation, respectively.

Figure 6 shows the voltage dependence of m_∞. The m_∞–V_m relationship curve was fitted to the following function:

$$P_{Ca}\, m_\infty = P_{Ca}[1+\exp((V_{m\frac{1}{2}}-V_m)/k)]^{-1}, \quad (4)$$

where $V_{m\frac{1}{2}}$ is the mid-point, V_m is the test-pulse potential and k is a measure of the steepness. The fitted parameters to this relationship in normal fibres were:

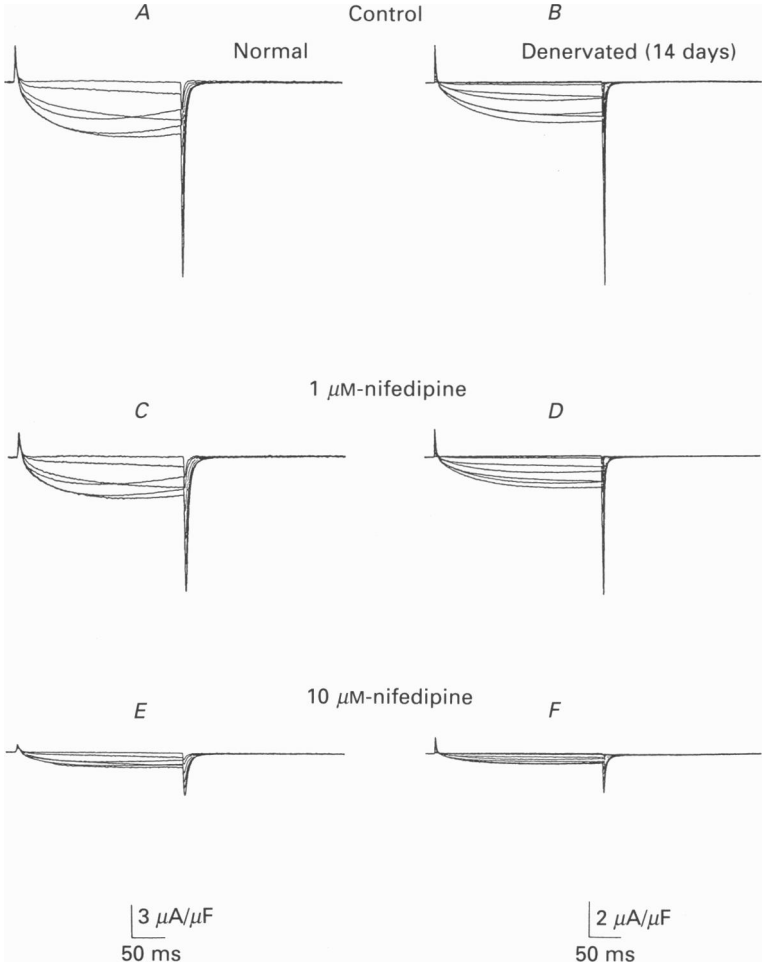

Fig. 7. Action of nifedipine on normal and denervated fibres. I_{Ca} records in two fibres, normal (*A*, *C* and *E*) and denervated (*B*, *D* and *F*) in control conditions and after incubating in 1 and 10 μM-nifedipine. The records were obtained by applying the *activation* pulse protocol. Only traces from −30 to 20 mV are depicted.

$V_{m\frac{1}{2}} = -4{\cdot}4$ mV and $k = 7{\cdot}6$ mV. During the first 4–6 days of denervation, the m_∞–V_m curve was not modified, with values of $V_{m\frac{1}{2}}$ and k of −7·9 mV (not significant, n.s.) and 6·5 mV (n.s.) respectively. At day 7 of denervation, the values of these parameters were −1·15 mV (n.s.) and 6·8 mV (n.s.) respectively. Between days 8 and 13 after denervation, the $V_{m\frac{1}{2}}$ was 1·1 mV ($P < 0{\cdot}05$) and the k value was 6·9 mV (n.s.).

Finally, at day 14 of denervation, the values of these parameters were 5·8 mV ($P < 0·05$) and 11·1 mV (n.s.) respectively. In summary, after denervation the steepness of the I_{Ca} activation was not modified while the half-activation potential was shifted to more positive potentials.

I_{Ca} sensitivity to nifedipine in denervated fibres

Figure 7 shows two control fibres, one corresponds to a normal fibre in control conditions (*A*), and the other to a 14-day-denervated fibre. In both groups, the fibres

TABLE 2. Nifedipine-sensitive I_{Ca}

	Nifedipine concentration	
Fibre type	1 μM	10 μM
Normal	0·25±0·02	0·74±0·03 (15)
Denervated (days)		
4–6	0·21±0·03	0·76±0·04 (10)
7	0·27±0·03	0·72±0·10 (10)
8–13	0·23±0·05	0·80±0·04 (10)
14	0·30±0·11	0·76±0·12 (10)

Values are means±S.E.M. Values in parentheses are the numbers of fibres. Values are expressed as $1-(I_{Ca}$ in nifedipine$/I_{Ca}$ control).

were tested with 1 (*C* and *D*) and 10 μM-nifedipine after 30 min incubation (*E* and *F*). The peak I_{Ca} was similarly reduced in both normal and denervated fibres. There was also a reduction of the charge movement induced by nifedipine (Ríos & Brum, 1987). The amounts of peak I_{Ca} reduction, expressed as $1-(I_{Ca}$ in nifedipine$/I_{Ca}$ control), by 1 and 10 μM-nifedipine are represented in Table 2. Student's *t* test was not significant in any of the denervated groups compared to control.

DISCUSSION

Criteria of denervation at the single fibre level

One of the first steps in this work was to design a procedure to discriminate between innervated and denervated fibres. A double-pulse protocol with variable interpulse V_h was developed for fibres incubated in I_{Ca} recording solutions as a test of denervation. This procedure avoids the use of nicotinic agonist, which can damage the fibre, to ascertain acetylcholine hypersensitivity and avoids the use of sodium current recording solutions, which prolongs the experiment, to ascertain TTX-resistant sodium current. In this I_{Ca} solution, I_{Na} was activated by shifting the V_h to more negative values than −90 mV. This outward current was carried by Na^+ ions since (i) the main internal cation was Na^+, (ii) the temporal course of this current was completed in no more than 3 ms, which argues against an I_K in spite of the proposed 4-aminopyridine and TEA resistance (Duval & Leoty, 1985), (iii) this current was insensitive to TTX and was not seen in normal fibres, (iv) the current was greatly reduced by replacing the internal sodium glutamate with caesium glutamate (data

not shown), and (v) after denervation there is a shift of the Na^+ current activation curve towards more negative potentials (Pappone, 1980).

Comparison of I_{Ca} activation in rat and frog fibres

An interesting difference between mammalian and frog skeletal muscle fibres is that frog fibres show a faster I_{Ca} activation with a pulse protocol as in Fig. 1. In rats, the time constant of I_{Ca} activation was not modified by this manoeuvre. Gating kinetics changes have been proposed to explain a faster onset of the I_{Ca} activation after different conditioning pulses (Feldmeyer, Melzer, Pohl & Zöllner, 1990; see also García, Ávila-Sakar & Stefani, 1990; Mejía-Alvarez *et al.* 1991). Furthermore, I_{Ca} from mammalian fibres is well fitted to an *mh* function (Delbono *et al.* 1991*a*; Mejía-Alvarez *et al.* 1991) while in frog muscle, the best fit is obtained with an m^3h function (Sánchez & Stefani, 1983).

Charge movement and I_{Ca} after denervation

In this study, charge movement was characterized in the absence of any drug that may potentially modify I_{Ca} and/or charge movement (Dulhunty & Gage, 1985; Lamb, 1986; Delbono *et al.* 1991*a*). The I_{Ca} amplitude increased during the first days of denervation and then decreased with respect to normal fibres. During the second week after denervation a significant reduction of the maximum charge movement was observed. The main question that arises from these observations is whether or not there is an actual reduction in the number of voltage sensors. It has been measured that the binding of labelled nitrendipine to rat muscle tissue increases after 3 days of denervation. This increase is followed by a slow drop of nitrendipine binding sites, but remains above control for more than 30 days (Schmid, Kazazoglou, Renaud & Lazdunski, 1984). The increase in nitrendipine binding sites (75%) (Schmid *et al.* 1984) is higher than the increase in peak I_{Ca} observed here (less than 50%) after the same period of denervation. It is known that depending on channel open probability the functioning channels could be much less than the channels detected by binding assays (Lamb & Walsh, 1987). The present study of charge movement would suggest that the number of DHP receptors decreases at later stages of denervation (two weeks).

Surface charge in denervated fibres

Changes in surface charges could be responsible for the shift in the voltage sensitivity of charge movement to more negative membrane potentials in denervated EDL fibres. In support of this hypothesis, some authors found that the time course of the change in the amount of charge movement in EDL fibres after denervation is similar to the time course of other structural changes in the sarcotubular membranes following denervation (Engel & Stonnington, 1974; Dulhunty & Gage, 1985), and other voltage-dependent processes are similarly affected such as a shift of Na^+ inactivation to more negative membrane potentials (Thesleff & Ward, 1975; Pappone, 1980). An increase of negative membrane charges after denervation (Blaise Smith & Appel, 1977) may at least partially account for the shift in mechanical threshold to more negative membrane potentials (Obejero Paz, Delbono & Muchnik, 1986; C. Obejero Paz & O. Delbono, unpublished). Thus, it would not be unlikely

that the shift of the $V_{q\frac{1}{2}}$ to the more negative membrane potential recorded in this work would be a consequence of an increase of negative surface charges. In support of this hypothesis the I_{Ca} inactivation is shifted to more negative membrane potentials (O. Delbono & E. Stefani, unpublished) but in conflict with this idea the I_{Ca} activation dependence was shifted to less negative membrane potentials during the second week after denervation.

Mechanical responses

Two types of modifications in prolonged mechanical responses have been recorded in denervated mammalian skeletal muscle, mainly a shortening of the potassium contractures rather than a considerable decrease in maximum force (Dulhunty & Gage, 1985) and a significant decrease of the maximum force of tetanic contractions (Finol *et al.* 1981; Kotsias & Muchnik, 1987). The former may be explained by a shift of the force inactivation curve to more negative membrane potentials or a reduction of the calcium affinity of the binding site for metal ions at the voltage sensor (Brum, Ríos & Stefani, 1988). The effect is comparable with the decrease in external Ca^{2+} concentration (Dulhunty & Gage, 1988).

Morphological and electrical changes

Fibres with smaller diameter have lower membrane capacitance because of the smaller contribution of the sarcotubular membrane (Hodgkin & Nakajima, 1972). After denervation histological changes occur (Dulhunty, Gage & Valois, 1984; Salvatori, Damiani, Zorzato, Volpe, Pierobon, Quaglino, Salviati & Margreth, 1989). The increase in the tubular membrane fraction gives rise to an increase in membrane capacitance in spite of a prominent decrease in fibre diameter. The increment in the volume fraction of the sarcotubular system (Engel & Stonnington, 1974) may account for the slowness of I_{Ca} activation after denervation. If the decrease in tubule entry resistance (since t-tubule diameter is increased) can render the sarcotubular membranes easier to clamp, then the time constant of I_{Ca} deactivation would appear to be faster than in normal fibres as was observed in this work. There is a parallel change in the numbers of indentations and the amount of charge movement after denervation, since the number of indentations in denervated EDL fibres were significantly lower than in normal muscles (Dulhunty *et al.* 1984). Alterations in Ca^{2+} channels themselves cannot be ruled out. The lack of modifications in nifedipine sensitivity after denervation does not rule out changes in Ca^{2+} channels, because the binding site to nifedipine is just a small part of the α_1-subunit of the channel (Catteral, 1988).

In summary, although the proliferation of the triads after denervation might explain a reduction of Ca^{2+} channels density, the present study suggests that there is an effective reduction of Ca^{2+} channels if currents are expressed in terms of membrane capacity. The reduction of voltage sensors detected by the reduction of charge movement and I_{Ca} amplitude at stages during denervation could account for the mechanical output failure in denervated mammalian skeletal muscle. The parallel reduction of charge movement and I_{Ca} lends support to the hypothesis regarding the molecular identity between the voltage sensor and DHP receptor (Ríos & Brum, 1987). An alternative explanation would be that I_{Ca} amplitude is normal

but charge movements had decreased after the first week of denervation. This assertion would find support in the shift to more negative potentials of the inactivation of other ionic currents studied in denervated muscle (Pappone, 1980), and preliminary results about I_{Ca} inactivation, that show a shift of the voltage dependence to more negative membrane potentials (O. Delbono & E. Stefani, unpublished).

This study was supported with grants from the National Institutes of Health (USA) (R01-AR38970) and Muscular Dystrophy Association (MDA) to Dr Enrico Stefani and a MDA fellowship to O.D. I am very grateful to Enrico Stefani, Alice Chu and Jesús García for their critical reading of the manuscript and helpful suggestions.

REFERENCES

BLAISE SMITH, P. & APPEL, S. H. (1977). Development of denervation alterations in surface membranes of mammalian skeletal muscle. *Experimental Neurology* **56**, 102–114.

BRUM, G., RÍOS, E. & STEFANI, E. (1988). Effects of extracellular calcium on calcium movements of excitation–contraction coupling in frog skeletal muscle fibres. *Journal of Physiology* **398**, 441–473.

CATTERAL, W. A. (1988). Structure and function of voltage-sensitive ion channels. *Science* **242**, 50–61.

CONTE CAMERINO, D., DE LUCA, A., MAMBRINI, M. & VRBOVA, G. (1989). Membrane ionic conductances in normal and denervated skeletal muscle of the rat during development. *Pflügers Archiv* **413**, 568–570.

COTA, G. & STEFANI, E. (1981). Effects of external calcium reduction on the kinetics of potassium contractures in frog twitch muscle fibres. *Journal of Physiology* **317**, 303–316.

DELBONO, O., GARCÍA, J., APPEL, S. H. & STEFANI, E. (1991*a*). Calcium current and charge movement of mammalian muscle: action of amyotrophic lateral sclerosis immunoglobulins. *Journal of Physiology* **444**, 723–742.

DELBONO, O., GARCÍA, J. & STEFANI, E. (1991*b*). Calcium current (I_{Ca}) in denervated single mammalian skeletal muscle fibers. *Biophysical Journal* **59**, 65a.

DELBONO, O. & KOTSIAS, B. A. (1991). Calcium action potentials in innervated and denervated rat muscle fibres. *Pflügers Archiv* **418**, 284–291.

DULHUNTY, A. F. & GAGE, P. W. (1985). Excitation–contraction coupling and charge movement in denervated rat extensor digitorium longus and soleus muscles. *Journal of Physiology* **358**, 75–89.

DULHUNTY, A. F. & GAGE, P. W. (1988). Effects of extracellular calcium concentration and dihydropyridines on contraction in mammalian skeletal muscle. *Journal of Physiology* **399**, 63–80.

DULHUNTY, A. F., GAGE, P. W. & VALOIS, A. A. (1984). Indentations in the terminal cisternae of denervated rat EDL and soleus muscle fibres. *Journal of Ultrastructure Research* **88**, 30–43.

DUVAL, A. & LEOTY, C. (1985). Changes in the ionic currents sensitivity to inhibitors in twitch rat skeletal muscles following denervation. *Pflügers Archiv* **403**, 407–414.

ENGEL, A. G. & STONNINGTON, H. H. (1974). Morphological effects of denervation of muscle. A quantitative ultrastructural study. *Annals of the New York Academy of Sciences* **228**, 68–88.

FELDMEYER, D., MELZER, W., POHL, B. & ZÖLLNER, P. (1990). Fast gating kinetics of the slow Ca^{2+} current in cut skeletal muscle fibres of the frog. *Journal of Physiology* **425**, 347–367.

FINOL, H. J., LEWIS, D. M. & OWENS, R. (1981). The effects of denervation on contractile properties in rat skeletal muscle. *Journal of Physiology* **319**, 81–91.

FRANCINI, F. & STEFANI, E. (1989). Decay of the slow calcium current in twitch muscle fibers of the frog is influenced by intracellular EGTA. *Journal of General Physiology* **94**, 953–969.

GARCÍA, J., AVILA-SAKAR, A. J. & STEFANI, E. (1990). Repetitive stimulation increases the activation rate of skeletal muscle Ca^{2+} currents. *Pflügers Archiv* **416**, 210–212.

GONOI, T. & HASEGAWA, S. (1988). Post-natal disappearance of transient calcium channels in mouse skeletal muscle: effects of denervation and culture. *Journal of Physiology* **401**, 617–637.

GUO, X., BRYANT, S. H. & MOCZYDLOWSKI, E. G. (1986). Tetrodotoxin-insensitive Na-channels from denervated rat muscle in planar lipid bilayers. *Biophysical Journal* **49**, 380a.

GUTMANN, E. & SANDOW, A. (1965). Caffeine-induced contracture and potentiation of contraction in normal and denervated rat muscle. *Life Sciences* **4**, 1149–1156.

HARRIS, J. B. & THESLEFF, S. (1971). Studies on tetrodotoxin resistant action potentials in denervated skeletal muscle. *Acta Physiologica Scandinavica* **83**, 382–388.

HENDERSON, L. P., LECHLEITER, J. D. & BREHM, P. (1987). Single channel properties of newly synthesized acetylcholine receptors following denervation of mammalian skeletal muscle. *Journal of General Physiology* **89**, 999–1014.

HODGKIN, A. L. & HUXLEY, A. F. (1952). A quantitative description of membrane current and its application to conduction and excitation in nerve. *Journal of Physiology* **117**, 500–544.

HODGKIN, A. L. & NAKAJIMA, S. (1972). The effect of diameter on the electrical constants of frog skeletal muscle fibres. *Journal of Physiology* **221**, 105–120.

IRVING, M., MAYLIE, J., SIZTO, N. L. & CHANDLER, W. K. (1987). Intrinsic optical and passive electrical properties of cut frog twitch fibers. *Journal of General Physiology* **89**, 1–30.

KOVÁCS, L., RÍOS, E. & SCHNEIDER, M. F. (1983). Measurements and modification of free calcium transients in frog skeletal muscle fibres by a metallochromic indicator dye. *Journal of Physiology* **343**, 161–196.

KOTSIAS, B. A. & MUCHNIK, S. (1987). Mechanical and electrical properties of denervated rat skeletal muscles. *Experimental Neurology* **97**, 516–528.

KOTSIAS, B. A. & VENOSA, R. A. (1987). Role of sodium and potassium permeabilities in the depolarization of denervated rat muscle fibres. *Journal of Physiology* **392**, 301–313.

LAMB, G. D. (1986). Components of charge movement in rabbit skeletal muscle: the effect of tetracaine and nifedipine. *Journal of Physiology* **376**, 85–100.

LAMB, G. D. & WALSH, T. (1987). Calcium currents, charge movement and dihydropyridine binding in fast- and slow-twitch muscles of rat and rabbit. *Journal of Physiology* **393**, 595–617.

LORKOVIC, H. (1985). Force and membrane potential in acetylcholine and potassium contractures of denervated mouse muscle. *Pflügers Archiv* **404**, 50–55.

MEJÍA-ALVAREZ, R., FILL, M. & STEFANI, E. (1991). Voltage-dependent inactivation of t-tubular skeletal calcium channels in planar bilayers. *Journal of General Physiology* **97**, 393–412.

OBEJERO PAZ, C., DELBONO, O. & MUCHNIK, S. (1986). Effects of actinomycin D on contractile properties of denervated rat skeletal muscle. *Experimental Neurology* **94**, 509–518.

PAPPONE, P. A. (1980). Voltage-clamp experiments in normal and denervated mammalian skeletal muscle fibres. *Journal of Physiology* **306**, 377–410.

REUTER, H. & SCHOLZ, H. (1977). A study of the ion selectivity and the kinetic properties of the calcium dependent slow inward current in mammalian cardiac muscle. *Journal of Physiology* **264**, 17–47.

RÍOS, E. & BRUM, G. (1987). Involvement of dihydropyridine receptors in excitation–contraction coupling in skeletal muscle. *Nature* **325**, 717–720.

SALVATORI, S., DAMIANI, E., ZORZATO, F., VOLPE, P., PIEROBON, S., QUAGLINO, D., SALVIATI, G. & MARGRETH, A. (1989). Denervation-induced proliferative changes of triads in rabbit skeletal muscle. *Muscle and Nerve* **11**, 1246–1259.

SÁNCHEZ, J. & STEFANI, E. (1983). Kinetic properties of calcium channels of twitch muscle fibres of the frog. *Journal of Physiology* **337**, 1–17.

SCHMID, A., KAZAZOGLOU, T., RENAUD, J. F. & LAZDUNSKI, M. (1984). Comparative changes of levels of nitrendipine Ca^{2+} channels, of tetrodotoxin-sensitive Na^+ channels and of ouabain-sensitive $(Na^+ + K^+)$-ATPase following denervation of rat and chick skeletal muscle. *FEBS Letters* **172**, 114–118.

SCHMID-ANTOMARCHI, H., RENAUD, J. F., ROMEY, G., HUGUES, M, SCHMID, A. & LAZDUNSKI, M. (1985). The all-or-none role of innervation in expression of apamin receptor and of apamin-sensitive Ca^{2+}-activated K^+ channel in mammalian skeletal muscle. *Proceedings of the National Academy of Sciences of the USA* **82**, 2188–2191.

THESLEFF, S. & WARD, M. R. (1975). Studies on the mechanism of fibrillation potentials in denervated muscle. *Journal of Physiology* **244**, 313–323.

WEISS, R. E. & HORN, R. (1986). Functional differences between two classes of sodium channels in developing rat skeletal muscle. *Science* **233**, 361–364.